Synergistic Effect on Crystalline Structure of Polyvinylidene Fluoride Nanocomposites with Multiwalled Carbon Nanotube Loading by a Twin Screw Extruder

Dong Jin Kang,[1,2] Kaushik Pal,[1] Dae Suk Bang,[2] Jin Kuk Kim[1]

[1]*Department of Polymer Science and Engineering, School of Nano and Advanced Materials Engineering, Gyeongsang National University, Gyeongnam, Jinju, 660-701, South Korea*
[2]*Department of Polymer Science and Engineering, Kumoh National Institute of Technology, Gumi, Gyeongbuk, 730-701, South Korea*

Received 28 May 2010; accepted 4 October 2010
DOI 10.1002/app.33524
Published online 17 February 2011 in Wiley Online Library (wileyonlinelibrary.com).

ABSTRACT: Polyvinylidene fluoride (PVDF)/multiwalled carbon nanotube (MWCNT) composites were prepared by using twin screw extruder at various (0–5 wt %) MWCNT loadings. Field Emission Scanning Electron Microscope (FESEM) micrographs showed a relatively good dispersion and random distribution of MWCNT in PVDF matrix. The physical and dielectric properties increased gradually with the increase in MWCNT content but the thermal stability decreased. The DSC result revealed the increase in crystallinity of the PVDF matrix. Wide angle X-Ray diffraction (WAXD) result showed a large shoulder at 2θ of 20.78° with increasing in MWCNT content. The experimental percolation threshold for the surface resistance of PVDF/MWCNT composites were estimated and clearly observed at 4 wt % of MWCNT loading. © 2011 Wiley Periodicals, Inc. J Appl Polym Sci 121: 226–233, 2011

Key words: nanocomposites; thermal analysis; electron microscopy; electrical properties

INTRODUCTION

Polyvinylidene fluoride (PVDF) and its polymeric composites have been extensively studied for piezoelectricity and dielectric property, since their electric properties were discovered in the past.[1–5] However, polymers are having low dielectric constant compared with ceramic and metal materials, generally used for high charge-storage capacitors, electrostriction system for artificial muscles and energy-storage devices. Consequently, a great deal of effort has been focused on the development of polymer/ceramic composites in which ferroelectric ceramics are selected as fillers to increase the dielectric constant of continuative polymers in the past several decades.[6,7] Polymer/ceramic composites have needed high loading of ceramic fillers in the composites; usually 50–60 vol % can increase dielectric constant by about ten times relative to the polymer matrix. This approach usually showed from the loss of the flexibility and the deterioration of processibility at the polymer composites.[8–10] It has been reported that CNTs can overcome these disadvantages, since not only a little concentrations of CNTs used but also easy to control the percolation behavior of the polymer/CNTs composites.[11–13]

Dielectric properties of PVDF were related with molecular and crystal structures, which may change depending on the preparation conditions of the stretching and poling system. The elongation of a PVDF film causes the orientation of chain molecules and the change of the crystal structure from α-form to β-form and poling system have suggested that the permanent dipole orientation can occur in the PVDF film.[1–5] The frequency-dependent dielectric constant, dielectric losses of PVDF and PVDF/MWCNT have been reported by many investigators. Bai et al. reported the dielectric constant of the ceramic/PVDF composites was about 250.[14] Wang and Dang reported that the dielectric constant of the pristine MWCNT/PVDF composites was 300.[15] Also recently, Li and Xue reported that the chemically purified MWCNT/PVDF was 3000.[16]

Variety of applications at polymer/CNTs composites strongly depends on the ability to disperse the CNTs homogenously throughout the matrix. However, the as-manufactured CNTs produced by

Correspondence to: K. Pal (pl_kshk@yahoo.co.in).
Contract grant sponsors: I-Cube Centre, Gyeongsang National University, Kumoh National Institute of Technology in South Korea.

Figure 1 4-kneeding screw configuration of twin screw extruder.

chemical vapor deposition (CVD) ordinarily exist as agglomerates of several hundred micrometers, which is an obstacle to most applications. Although a number of studies have been focused on dispersion of CNTs in polymers, complete dispersion of CNTs in a polymer matrix remains elusive. Most researchers have been focused on chemical modification of the CNTs to improve dispersion through functionalization.[17,18] Chemical modification may improve efficiency of load transfer between the polymer matrix and the CNT's, however, it also introduces defects on the carbon–carbon bonding in CNT networks and CNTs walls, which will lower their inherent properties such as, electrical and thermal conductivity. Other researchers have also investigated about some physical dispersion methods, include ultrasonication, ball milling, grinding and high speed shearing of CNT into the matrix. Also, it has been proved that physical dispersion methods not only separate CNT agglomerates, but also fragment the nanotubes.[19,20]

In this article, PVDF/MWCNT composites were fabricated by very simple and effective route by a twin screw extruder with excellent physical, thermal, electrical, and dielectric properties of stretching and nonstretching with poled film for large scale application in aerospace and electro device industry.

EXPERIMENTAL

Materials and sample preparation

A commercially available polyvinylidene fluoride powder (SOLEF 1015, T_m = 173°C, MI = 0.2) was supplied by Solvay, Inc. (Belgium) and high purity multiwall carbon nanotubes having diameter in the range of 10–30 nm, lengths between 10 and 20 μm, and purities of more than 95% were supplied by ILJIN Nanotech Co. (Republic Korea). PVDF was dried at 60°C in a dry oven for 3 h before use. After that, PVDF and MWCNT powders were premixed before a melt compounding, using a high speed mixer (Waring products, USA) for 2 min at 2000 rpm. Powder PVDF was mixed with MWCNT from 1 to 5 wt % of loading. PVDF/MWCNT composites were prepared via a melt compounding method using a modular intermeshing corotating twin screw extruder manufactured by Bautech Co. It was composed with a barrel of 11 mm in diameter and L/D ratio of 41. The barrel temperature, from the hopper to the die, was 150-170-190-190-190-180°C. 4-kneading screw configuration which has reverse screw elements and kneading element positioned and shown in Figure 1 was used for intermixing. Film samples (with thickness of about 0.2 mm) were prepared by compression molding machine at a temperature of 200°C with a pressure of 13.8 MPa.

Corona poling preparation

To provide the piezoelectric property, both the DC contact and the corona poling method were employed. In the corona poling method, a 940 μm diameter copper wire was used as an electrode to generate the corona discharge. The distance between the copper wire and the film is kept at 2 cm, and the applied DC voltage between the copper wire and the copper electrode was about 10 kV. While the corona discharge was being sustained, the poling current fluctuated minutely between 0.32 and 0.03 mA. In the DC contact poling method, room temperature was essential to avoid severe degradation of the electrode and the film. A copper electrode of 50 μm in thickness was used for deposited on the film surface in vacuum, and a DC voltage was applied while the film was being cured at an elevated temperature.

Characterization

A Field Emission Scanning Electron Microscopy (FE-SEM) was performed by JEOL JSM-6500F. It was used to observe the morphology of the cryo fractured surfaces (fractured by mechanical force) of PVDF/MWCNT nanocomposites. Samples were sputtered with gold-palladium prior to testing. Thermogravimetric analysis (TGA Q500, TA Instruments) was carried out to study the thermal stability of PVDF/MWCNT nanocomposites. The sample of 20 $\sim$ 25 mg was heated under nitrogen atmosphere from room temperature to 600°C at a heating rate of 10°C min^{-1}. Differential Scanning Calorimetry (DSC) was performed on PVDF melt-compound samples using a DSC 300 F3 (NETZSCH, Germany). Heat flow was monitored over the range of 50–220°C with temperature modulation (±0.8°C every 60 s) superimposed on a 10°C min^{-1} heating and cooling rate. All samples were placed in a crimped aluminum pan typical to the reference pan in size, approximately 10 $\sim$ 12 mg in weight. Experimental runs were done under purge gas (nitrogen at 50 mL min^{-1}). Dynamic mechanical analysis (DMA Q800, TA Instruments) was done by purging liquid nitrogen gas with a heating rate of 5°C min^{-1} at a fixed frequency of 1 Hz, with oscillation amplitude of 0.2 mm in tension mode. The specimen dimensions

were 20 mm × 5.3 mm × 0.2 mm. X-Ray Diffraction (XRD) study was performed on the samples using WAXD machines. The β-phase and α-phase control samples were measured on a Rigaku X-ray diffractrometer. The surface resistance measurement was performed in the range between 10^3 Ω/square and 10^{14} Ω/square using MEGOHM METER (ACL 800, USA). The resistivity of PVDF/MWCNT composites having dimension 10 × 50 × 0.21 mm^3, were measured at room temperature using two-probe grip type. For each sample, data was measured at least five times and averaged. The dielectric measurements were carried out using a programmable automatic impedance analyzer (Agilent E4294A) in the frequency range from 1 KHz to 10 MHz. The cell was calibrated using air and Teflon sheet as standard references. The frequency and bias dependence of the real and imaginary parts of the complex dielectric permittivity has been studied in detail at room temperature. The dielectric properties of the PVDF/MCWNT were taken at off voltages.

RESULTS AND DISCUSSION

Morphology

FE-SEM microphographs of fractured surface of pristine PVDF and PVDF/MWCNT nanocomposites are presented in Figure 2. In Figure 2, composites having 1–4 wt % of MWCNTs loading show the good dispersion and distribution in the matrix, despite of some aggregation in the matrix. However, the composite with 5 wt % of MWCNT loading shows some poor dispersion and distribution properties of MWCNT rather than other composites and are observed to be 70 ∼ 100 nm in diameter. That is mainly occurred due to the use of high MWCNT concentrations and those are lumped together by Vander-Waals force and interrupt the mobility of polymer molecules. Also, these retained and undistributed MWCNT's in polymer matrix are responsible to higher the viscosity of PVDF matrix.

Thermal properties (TGA, DSC)

Figure 3 shows the TGA thermograms of PVDF/MWCNT composites with various concentrations of MWCNT, at a heating rate of 10°C/min in N_2 atmosphere. The onset degradation temperature of PVDF is around 440°C and it is completely decomposed at 520°C, and the weight loss of PVDF at 600°C is negligible. The degradation temperature of PVDF/MWCNT composites is getting lower with the increasing concentration of MWCNT. It is usually accepted that the improved thermal stability for exfoliated nanocomposites is mainly due to the formation of char, which hinders the diffusion of the volatile decomposition products, as a direct result of the improved permeability.[21] However, in some cases the poor dispersion and distribution of nanocomposites lead to regional insufficient char formation than the exfoliation, probably due to the high level of MWCNT loading.[22]

With relation to the residual portion for temperatures between 450 and 600°C, the residual weight is higher for the composites containing MWCNT, than pristine PVDF. Apparently the MWCNT present as additive seem to make the degradation kinetics slower upon absorbing the heat during the degradation process.[23]

The heating scan thermograms of PVDF and PVDF/MWCNT composites are shown in Figure 4(a). All the samples produced a main melting peak at around 172°C. With the presence of MWCNT, main melting peak does not shift severely; it seems almost same as pristine PVDF. However, the addition of MWCNT more than 4 wt % produces the shoulder posterior to the main melting peak and an increased in end point of the peak. This phenomenon is attributed to the presence of two morphologically different crystallites. Data from the literature supports the idea that the double melting peaks observed in the DSC experiment on PVDF are due to a peculiar polymorphic structure of this polymer.[24,25] In particular, some literature depicted that the low temperature melting peak was due to the formation of α-form crystalline structure while the high temperature peak is due to the β-form. The β-phase crystal with all-trans conformation gives higher endotherm than the α-phase crystal with *trans*-gauche-*trans*-gauche (TGTG) conformation.[23] This is a good agreement with WAXD results. On the other hand, as shown in Figure 4(b), up to 1 wt % loading of MWCNT, it has little effect on the crystallization temperature of PVDF, but further addition of MWCNT loading T_c values increases from 141.6 to 143.7°C. This suggests that MWCNT acts as a nucleation agent for PVDF above a critical loading level in this study.

Dynamic mechanical properties

Figure 5 shows the DMA plot in which the temperature dependence of the dynamic storage modulus and the storage modulus at 50°C (the inset) are presented as a function of MWCNT concentration. It can be seen that the storage moduli of the composites increase abruptly. As the MWCNT loading increases from 1 to 5 wt %, there is a significant increase in the storage modulus by 80% than the virgin PVDF. Even at temperature well above the room temperature, for instance, at 100°C, the increase in modulus is about 30% for the composite containing only 5 wt % MWCNT. The significant improvement

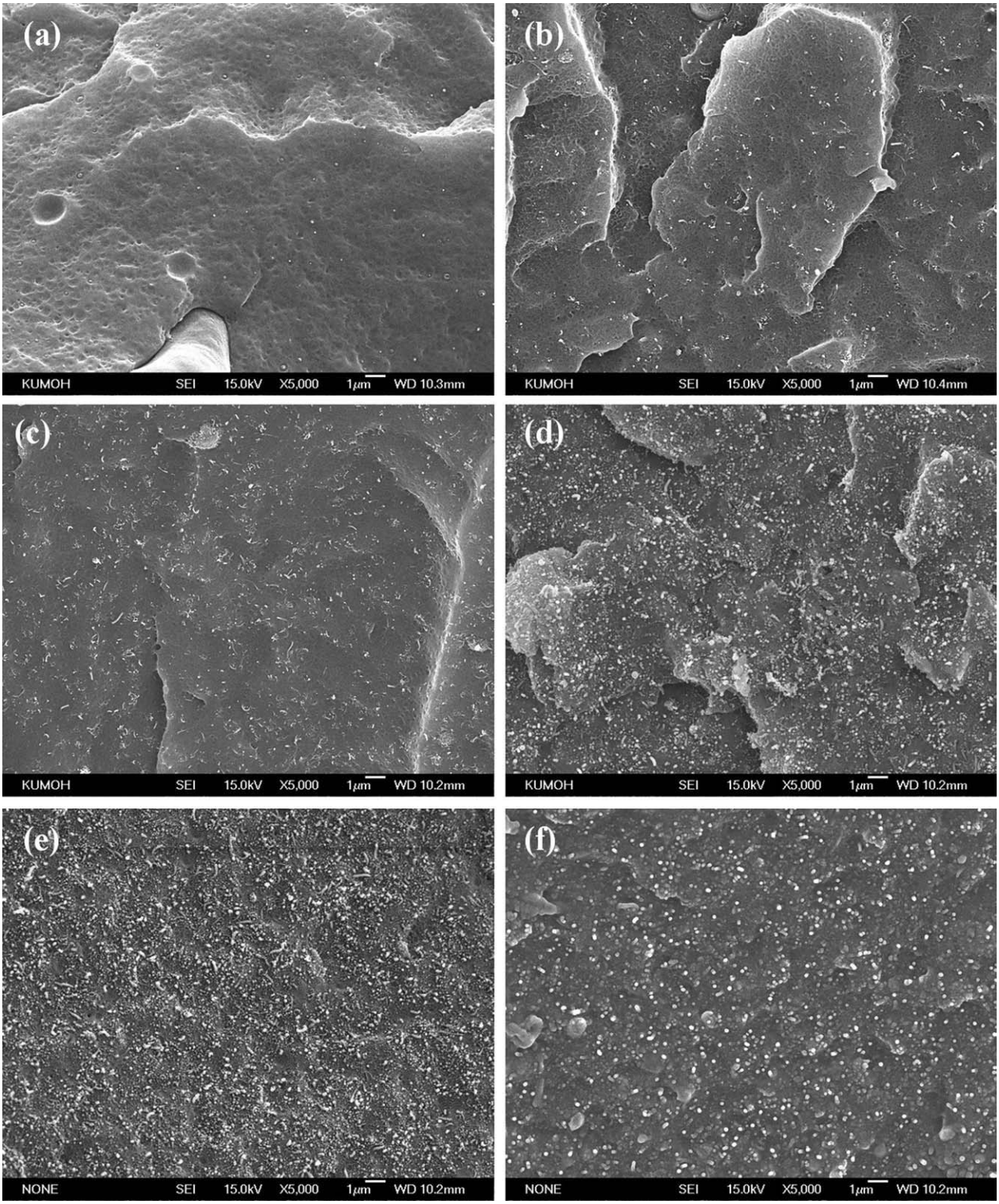

Figure 2 SEM images of fracture surface of PVDF/MWCNT nanocomposites, (a) pristine PVDF (b) 1 wt % MWCNT (c) 2 wt % MWCNT (d) 3 wt % MWCNT (e) 4 wt % MWCNT (f) 5 wt % MWCNT.

in the storage modulus at temperature higher than the glass transition temperature, $T_g = -50°C$, of PVDF clearly confirms the reinforcing effect of MWCNT in the composites.[26,27]

Generally, the augmentation of storage modulus on increasing filler content can be attributed to the hydrodynamic effect of filler particle embedded into the polymer matrix. It has been suggested that there

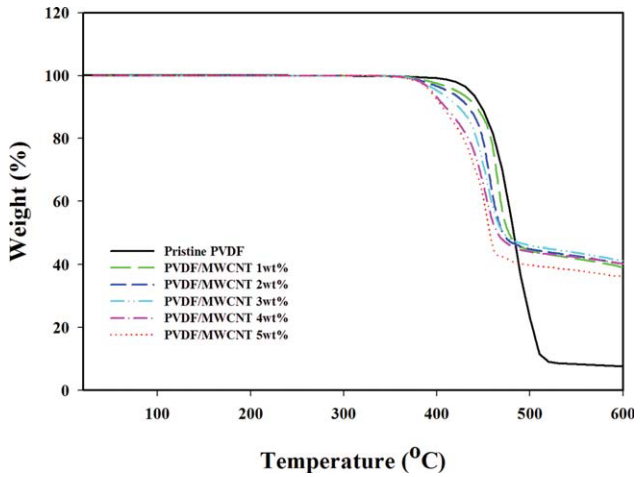

Figure 3 TGA thermograms of pristine PVDF and PVDF with 1, 2, 3, 4, and 5 wt % MWCNT. [Color figure can be viewed in the online issue, which is available at wileyonlinelibrary.com.]

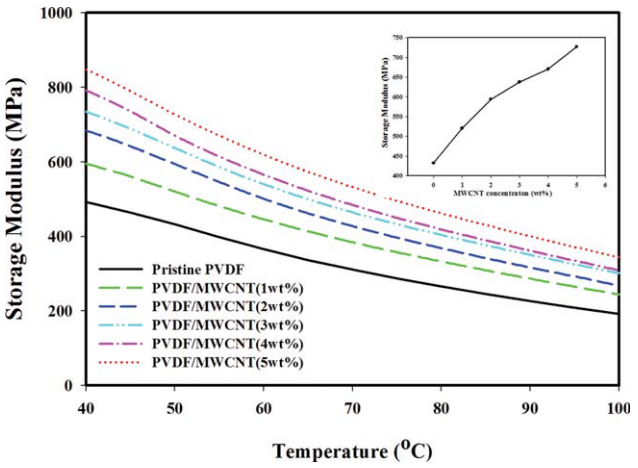

Figure 5 Temperature dependence of the storage modulus for PVDF and its nanocomposites. The inset shows storage modulus variation with wt % of MWCNT. [Color figure can be viewed in the online issue, which is available at wileyonlinelibrary.com.]

are three components in filled polymer samples distinguished by their characteristic molecular mobility: immobilized fraction, intermediate fraction, and mobile fraction.[28] The immobilized fraction is the polymer that is immobilized on the filler surface. It is trapped by the filler particles, such that its dynamics are influenced by the proximity of the filler surface. The mobile fraction increases further from the filler loadings such that the motions are not restricted and it has the characteristics of polymers. So, with increasing content of MWCNT in the composites, more and more polymer chains are expected to attach and to be in the vicinity of the filler surface. Also, with increasing temperatures, the free volume of the polymer increases leading to relaxation of the polymer chains and consequently increasing the modulus.

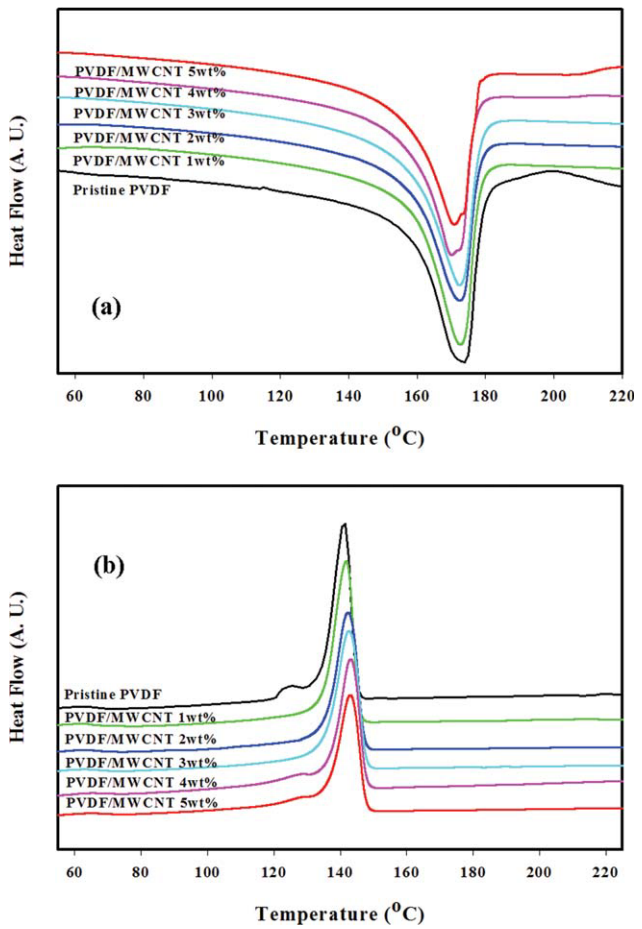

Figure 4 DSC thermograms of pristine PVDF and PVDF with 1, 2, 3, 4, and 5 wt % MWCNT. (a) 1st heating scan, (b) 1st cooling scan. [Color figure can be viewed in the online issue, which is available at wileyonlinelibrary.com.]

Waxd patterns of PVDF and composites

WAXD is used to observe the effect of MWCNT content on the microstructure of pristine PVDF. Figure 6(a) describes the WAXD patterns for pristine PVDF and PVDF/MWCNT nanocomposites. Within a given range of scattering angles, three characteristic diffraction peaks appear at 2θ value of 17.7, 18.4, and 19.9° respectively, which correspond to (100), (020), and (110) reflections, respectively. This is assigned to the α-phase crystal which has a nonpolar *trans*-gauche-*trans*-gauche (TGTG) conformation.[23] PVDF/MWCNT nanocomposites exhibit decrease in peaks for α-phase crystal for 1 wt % MWCNT loading. In addition to the features associated with β-phase crystal, the introduction of MWCNT produces a shoulder at a 2θ value of 20.7° and it is clear with increasing the MWCNT content also. This is attributed to the formation of β-phase crystal which has all-trans conformation. As one can observe, the incorporation of the filler causes a reduction in the intensity of the α-phase characteristic peaks,

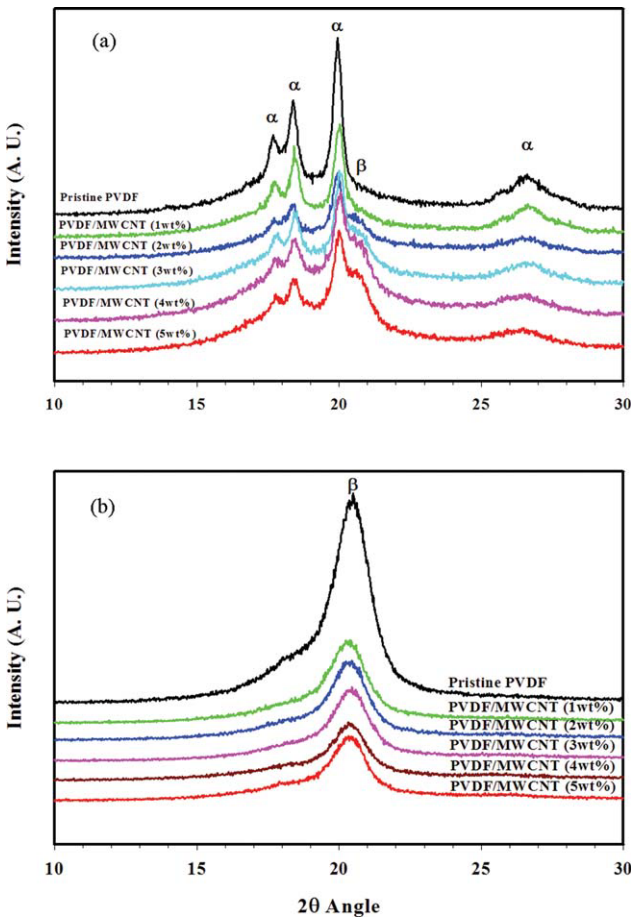

Figure 6 WAXD patterns of (a) pristine PVDF and PVDF/MWCNT nanocomposites and (b) change of the crystal structure from α-phase crystal form to β-phase crystal. [Color figure can be viewed in the online issue, which is available at wileyonlinelibrary.com.]

especially for the peak at 26.5°. Also, this effect is more remarkable for MWCNT.[29] In the extreme case of the PVDF/MWCNT composite, such effect is very clear. Figure 6(b) shows drawing of a PVDF film causes the orientation of chain molecules and the change of the crystal structure from α-phase crystal form to β-phase crystal conformation.

Surface resistance

Electric property investigates the effect of MWCNT content on the surface resistance of PVDF. The variation in electrical conductivity of PVDF, filled with MWCNT is given in Figure 7 as a function of the MWCNT content in the polymer matrix. The surface resistance of the PVDF composites is proportionally depending on the content of MWCNT (conductivity of MWCNT: 75 S/cm). The surface resistance is increased from 10^{14} to 10^{3} S/cm with increasing content of MWCNT from 1 to 5 wt %.

Surface resistance shows the typical percolation behavior for PVDF/MWCNT nanocomposites at 4 wt % of MWCNT content and as shown in Figure 7. This indicates that a nanotube network in the polymer matrix forms from the percolation content. However, above 4 wt % of MWCNT loading, additional incorporation of MWCNT does not significantly alter the surface resistance, which is a measure of long range movements of charge carrier. This indicates that there is conductivity saturation from a critical content because of formation of an infinite cluster.[28]

Dielectric properties

Dielectric spectroscopy is performed on the PVDF/MWCNT nanocomposites to determine the changes in the electric properties of the composite occurring after the addition of different concentrations of MWCNT. Dielectric constants are improved with increasing the content of MWCNT. Dielectric constant (ε′) measurements are taken at room temperature. Dielectric dissipation (loss tanδ) is measured as a function of frequencies shown in Figures 8 and 9. These are improved with increasing the content of MWCNT. Ionic conduction phenomena are slightly observed above 4 wt % of MWCNT. These results implied that the PVDF resin filled with MWCNT could be prospective actuator, super capacitor material since can enhance the conductivity and permittivity by controlling the content of MWCNT. Also, the dissipation energy is decreasing with increase in frequency but at higher frequencies it is almost constant. According to Debey's theory, the decreasing of viscosity between dipole and neighboring medium in accordance with increase of temperature affected reduce the relaxation time of permanent dipole, so that dielectric absorption moves to high frequency.[16]

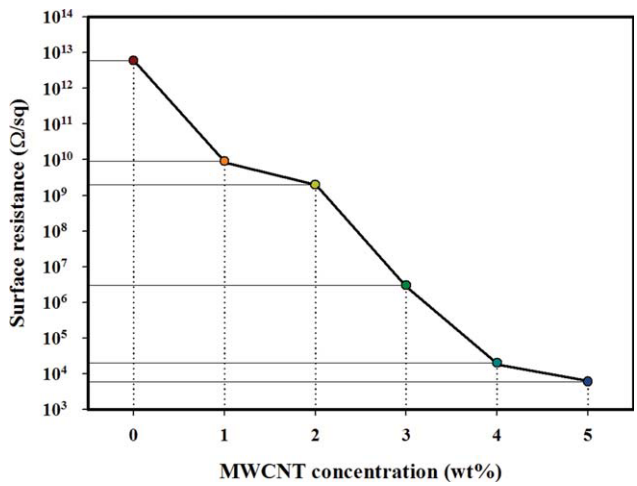

Figure 7 Variation of the surface resistance of pristine PVDF and PVDF/MWCNT composites with MWCNT contents. [Color figure can be viewed in the online issue, which is available at wileyonlinelibrary.com.]

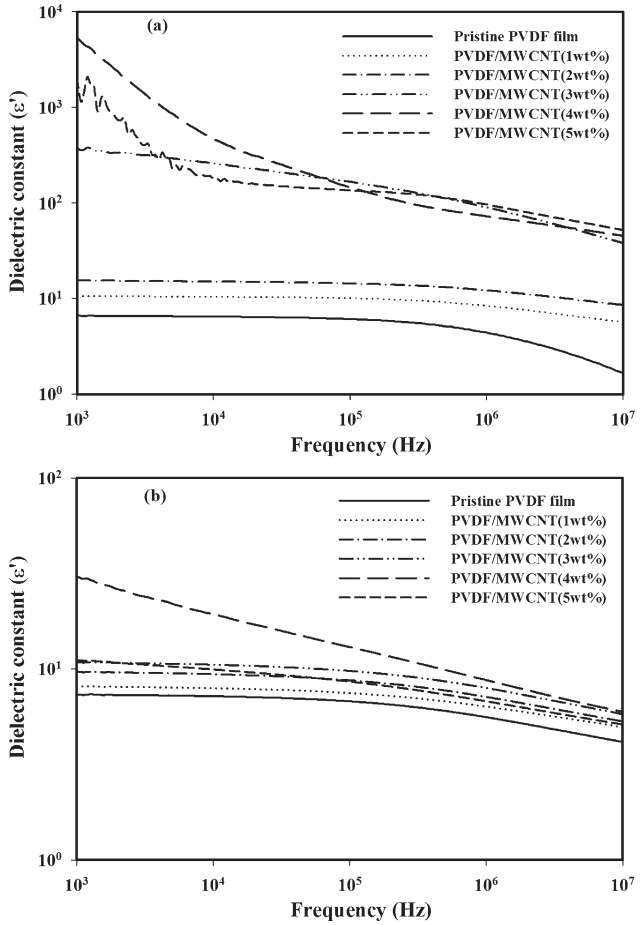

Figure 8 Frequency dependence of (a) non stretch and (b) stretch dielectric constant of the PVDF/MWCNT nanocomposites.

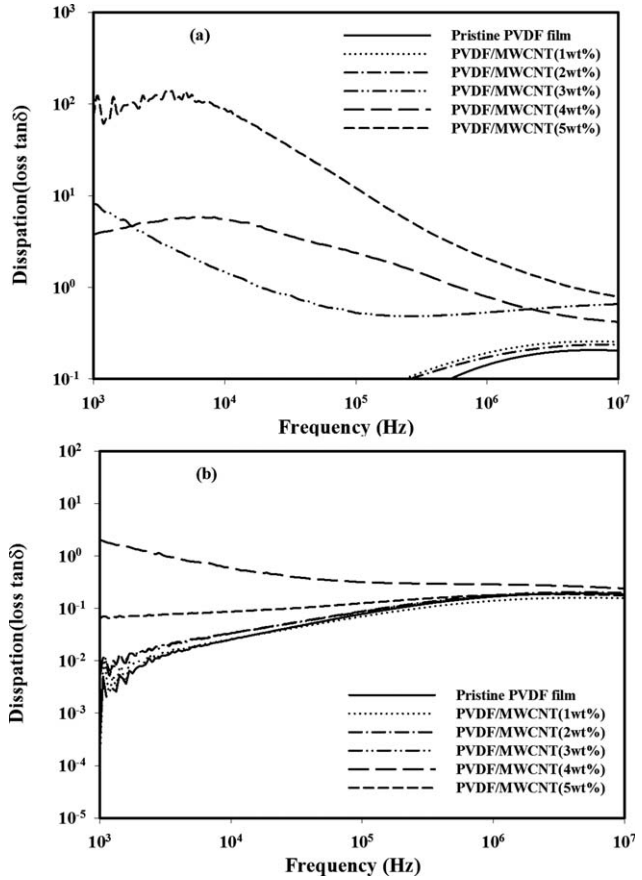

Figure 9 Frequency dependence of (a) nonstretch and (b) stretch dissipation of the PVDF/MWCNT nanocomposites.

Dielectric properties show two interesting results in this study. First, the dielectric constant of the stretched PVDF/MWCNT nanocomposites film is lower than unstretched film. However, according to other works, the crystal form of PVDF transferred from α-form to β-form which is responsible for increase in dielectric constant. This is happened because MWCNT involved into the defects of crystallization and make void in polymer surface thus surface resistance is increased. Because of the destroyed network structure of MWCNT, this led to the dielectric constants decrease during drawing. Second, it is observed that for MWCNT/PVDF film, the dissipation as well as dielectric constant decreased with increase in frequency, while for pristine PVDF, the dissipation energy increase.

CONCLUSIONS

In this study, high viscosity of PVDF and PVDF/MWCNT are successfully extruded with different MWCNT concentration. In the results, FE-SEM micrographs show relatively good dispersion of MWCNT in PVDF and random distribution. The results from thermal properties of the composites show that increase of the melting point temperature due to change in crystal formation from α-phase to β-phase with increasing content of MWCNT. It proves that due to the increase in MWCNT concentration, T_c shifts to the higher temperature side, because MWCNT works as a nucleation site in the polymer molecules. Also, the storage modulus increases upto 80% when MWCNT concentration increases from 1 to 5 wt %, according to DMA results. WAXD results show a shoulder at a 2θ value of 20.7° due to the presence of MWCNT and this β-form is more prominent with increase in MWCNT contents. Surface resistance analysis shows the typical percolation behavior for PVDF composites with 4 wt % MWCNT content. This indicates that a nanotube network in the polymer matrix forms from the percolation content. However, above 4 wt %, additional incorporation of MWCNT does not significantly alter the surface resistance. The increase in the dielectric constant of PVDF/MWCNT nanocomposites is due to the conductive properties of the MWCNT. The increase in the dielectric constant allows the material to carry more current and energy to the piezoelectric dipoles, which improves the

material's piezoelectric effects resulting in a better capacitors or actuator properties.

References

1. Kawai, H. Jpn J Appl Phys 1969, 8, 975.
2. Furukawa, T.; Aiba, J.; Fukada, E. J Appl Phys 1979, 5, 50.
3. Ho, C. H.; Liu, C. D.; Hsieh, C. H.; Hsieh, K. H.; Lee, S. N. Synthetic Metal 2008, 158, 630.
4. Dang, Z. M.; Nan, C. W. Ceram Int 2005, 31, 349.
5. Singh, R.; Kumar, J.; Singh, R. K.; Kaur, A.; Sinha, R. D. P.; Gupta, N. P. Polymer 2006, 47, 5919.
6. Park, J. M.; Kim, S. J.; Jang, J. H.; Wang, Z.; Kim, P. G.; Yoon, D. J.; Kim, J.; Hansen, G.; DeVries, K. L. Compos B 2008, 39(7–8), 1161.
7. Moussaif, N.; Groeninckx, G. Polymer 2003, 44, 7899.
8. Ying, Z.; Jiang, Y.; Du, X.; Xie, G.; Yang, Y. J Appl Polym Sci 2007, 106, 1024.
9. Zucolotto, V.; Avlyanov, J.; Gregorio, R., Jr.; Mattoso, L. H. C. J App Polym Sci 2004, 94, 553.
10. Kobayashi, Y.; Tanase, T.; Tabata, T.; Miwa, T.; Konno, M. J Euro Cer Soc 2008, 28, 117.
11. Tran, M. Q.; Shaffer, M. S. P.; Bismarck, A. Macromol Mater Eng 2008, 293, 188.
12. Seema, A.; Dayas, K. R.; Varghese, J M. Carbon 2007, 45, 2334.
13. Koerner, H.; Price, G.; Pearce, N.; Alexander, M.; Vaia, R. A. Nat Matls 2004, 3, 115.
14. Bai, Y.; Cheng, Z. Y.; Bharti, V.; Xu, H. S.; Zhang, Q. M. Appl Phys Lett 2000, 76, 3804.
15. Wang, L.; Dang, Z. M. Appl Phys Lett 2005, 87, 042903-91-3.
16. Li, Q.; Xue, Q.; Zheng, Q.; Hao, L.; Gao, X. Mater Lett 2008, 62, 4229.
17. Park, C.; Ounaies, Z.; Watson, K.; Crooks, R.; Smith, J.; Lowther, S., Jr.; Connell, J.; Siochi, E.; Harrison, J.; Clair, T. St. Chem Phys Lett 2002, 364, 303.
18. Weber, M.; Kamal, M. Polym Compos 1997, 18, 711.
19. Shaffer, M. S. P.; Fan, X.; Windle, A. H. Carbon 1998, 36, 1603.
20. Potschke, P.; Bhattacharyya, A. R.; Janke, A. Eur Polym Mater 2004, 40, 137.
21. Alexandre, M.; Dubois, P. Mater Sci Eng Res 2000, 28, 1.
22. Gilman, J. W. Appl Clay Sci 1999, 15, 31.
23. Pramoda, K.; Mohamed, A.; Phang, I. Y.; Liu, T.; Polym Int 2005, 54 226.
24. Maraga, C.; Marigo, A. Eur Polym J 2003, 39, 1713.
25. Madorskaya, L. Y.; Samoilov, V. M.; Otradina, G. A.; Agapitov, A. P.; Budtov, V. P.; Makeyenko, T. G.; Kharcheva, Y. Y.; Loginova, N. N. Polym Sci USSR 1984, 26, 2891.
26. Esterly, D. M.; Love, B. J. Polym Sci Part B: Polym Phys 2004, 42, 91.
27. Priya, L.; Jog, J. P. Polym Sci, Part B: Polym Phys 2002, 41, 31.
28. Kenny, J. C.; Briety, M. C.; Rigbi, V. J. Z.; Douglass, D. C. Macromolecules 1991, 24, 436.
29. Hong, S. M.; Nam, Y. W.; Sang, S. H.; ChaeD. W. Mol Cryst Liq Cryst 2007, 464, 195.